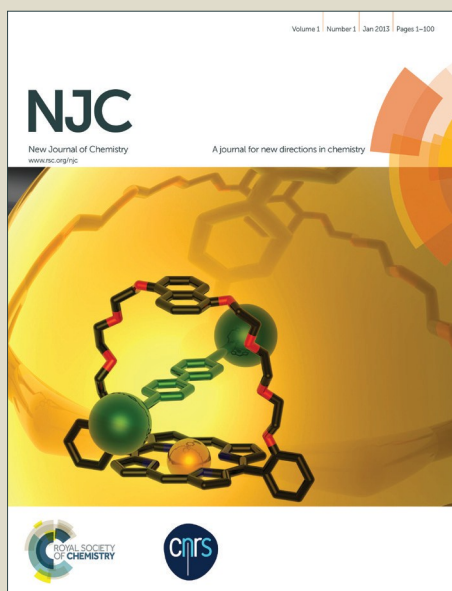


NJC

Accepted Manuscript



This is an *Accepted Manuscript*, which has been through the Royal Society of Chemistry peer review process and has been accepted for publication.

Accepted Manuscripts are published online shortly after acceptance, before technical editing, formatting and proof reading. Using this free service, authors can make their results available to the community, in citable form, before we publish the edited article. We will replace this *Accepted Manuscript* with the edited and formatted *Advance Article* as soon as it is available.

You can find more information about *Accepted Manuscripts* in the [Information for Authors](#).

Please note that technical editing may introduce minor changes to the text and/or graphics, which may alter content. The journal's standard [Terms & Conditions](#) and the [Ethical guidelines](#) still apply. In no event shall the Royal Society of Chemistry be held responsible for any errors or omissions in this *Accepted Manuscript* or any consequences arising from the use of any information it contains.

Interaction of ruthenium (II) antitumor complexes with d(ATATAT)₂ and d(GCGCGC)₂ : A theoretical study

Dharitri Das, Paritosh Mondal*

Department of Chemistry, Assam University, Silchar 788011, Assam, India

*Corresponding author. Email: paritos_au@yahoo.co.in

Abstract

Interaction of three ruthenium (II) complexes of the type [Ru(tmp)₂(dpq)]²⁺ (**I**), [Ru(tmp)₂(dppz)]²⁺ (**II**) and [Ru(tmp)₂(11,12-dmdppz)]²⁺ (**III**) with two B-DNA hexamers of alternative AT and GC sequences, namely d(ATATAT)₂ and d(GCGCGC)₂ respectively, has been computationally investigated by the molecular docking and two layer quantum mechanics/molecular mechanics hybrid method. Docking simulation reveals the intercalative minor groove binding mode of ruthenium complexes with DNA base pairs as well as their preferential binding to d(ATATAT)₂ over d(GCGCGC)₂. In addition, docking simulation exhibits the greater binding affinity of complex **III** toward the DNA sequences compared to complexes **I** and **II**, which indicates that methyl substituent effect of the intercalating ligand increases the binding affinity towards DNA duplex. Binding energies of ruthenium complexes with DNA sequences obtained from two layer quantum mechanics/molecular mechanics calculation show higher stability of **III-DNA** adduct as compared to the adducts of complexes **I** and **II** with DNA. The stability order for ruthenium (II) complexes with d(ATATAT)₂ and d(GCGCGC)₂ sequences are as follows: complex **III** > complex **II** > complex **I**. Thus molecular docking and quantum mechanics/molecular mechanics results express that intercalating ligand having substituent group significantly increases the DNA binding affinity of the metal complexes.

Keywords: DFT, ruthenium (II) complexes, Docking, ONIOM

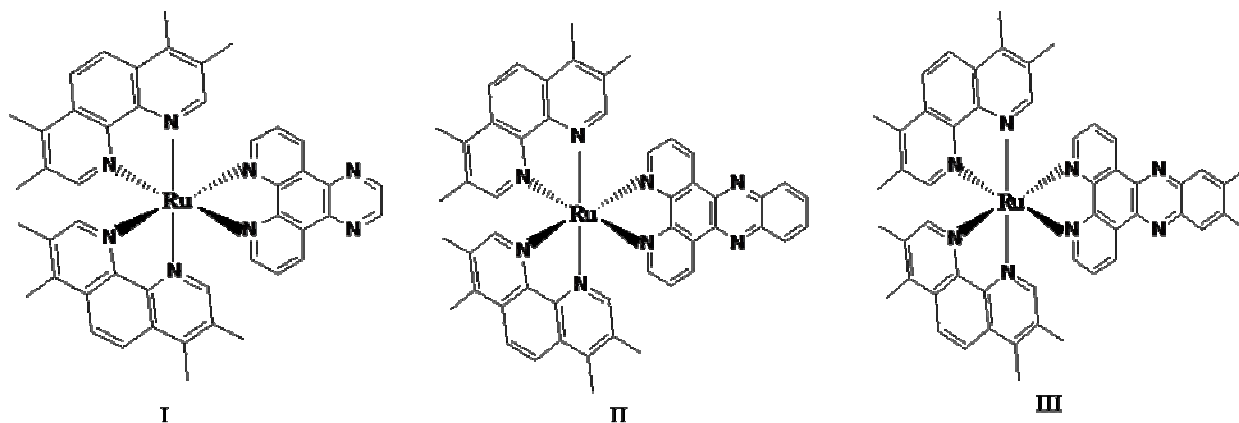
1. Introduction

DNA becomes an important cancer target in the design of novel chemotherapeutics to block the replication step in the cell cycle. Even though the inhibition of DNA replication is not new in cancer therapy, the use of novel chemical reagents are still desirable to improve the effects of treatment, particularly by reducing the occurrence of drug side effects and resistance.¹⁻³ Biological activity occurs due to the covalent and non-covalent interactions of transition metal complexes with DNA.⁴⁻⁵ Last decade has seen a series of transition metal complexes that have been used as DNA cleaving agents.⁶⁻¹² However, DNA cleavage by polypyridyl ruthenium (II) complexes have been the focal point of several research works. Ruthenium (II) polypyridyl complexes have received a great deal of attention because of their stability, ease of construction, chirality, opto-electronic properties, strong binding affinity to DNA and luminescence characteristics.^{6-9,13} Barton *et al.*¹⁴ was among the first group that had analyzed the interactions of positively charged transition metal complexes with DNA. $[\text{Ru}(\text{phen})_3]^{2+}$ (binding constant of 10^3 M^{-1}) can bind to DNA through three non-covalent modes namely; electrostatical, hydrophobic or by partial intercalation of the phenanthroline ligand into DNA.¹³ On the other hand, Ericksson *et al.* have reported that both Δ and Λ enantiomer of $[\text{Ru}(\text{phen})_3]^{2+}$ complex bind to DNA only through intercalative mode.¹⁵ Intercalative binding is defined as the non covalent stacking interaction occurring due to the insertion of a planar heterocyclic aromatic ring between base pairs of DNA double helix.¹⁶ $[\text{Ru}(\text{bpy})_2(\text{dppz})]^{2+}$ (bpy=2, 2'-bipyridine) and $[\text{Ru}(\text{phen})_2(\text{dppz})]^{2+}$ (phen=1,10-phenanthroline), are the prototype of DNA intercalators that contain a DNA intercalating ligand namely dipyrrodo [3,2-a: 2', 3'-c] phenazine (dppz).¹⁷⁻¹⁸ Based on recent crystallographic study conducted in Barton and Lincoln laboratory, the Δ -enantiomer of $[\text{Ru}(\text{bpy})_2\text{dppz}]^{2+}$ have been found to intercalate into the minor groove at CG/CG and AT/AT, resulting DNA cleavage.¹⁹⁻²² The $[\text{Ru}(\text{bpy})_2(\text{dppz})]^{2+}$ displayed an extremely high affinity for CT DNA, having a binding constant of 10^6 M^{-1} , which suggested that an increase in surface area of bridging ligand can significantly increase the DNA binding affinity.¹⁷ On the other hand, according to Hall *et al.* both Λ - and Δ -enantiomer of $[\text{Ru}(\text{phen})_2\text{dppz}]^{2+}$ shows intercalation from the minor groove of DNA.²³ Erkkila *et al.* have carried out systematic study on rac- $[\text{Ru}(5,6\text{-dmp})_3]^{2+}$ / rac- $[\text{Ru}(\text{phen})_3]^{2+}$ complexes and observed that presence of 5,6-dimethyl-

1,10-phenanthroline ligand enhances the binding affinity of $\text{rac- [Ru(5,6-dmp)}_3\text{]}^{2+}$ with DNA receptor than $\text{rac-[Ru(phen)}_3\text{]}^{2+}$ complex.²⁴ On studying binding affinity of several osmium (II) tris-complexes of methyl substituted and unsubstituted 1,10-phenanthrolines with DNA, Maruyama and his co-workers reported that $[\text{Os(5,6-dmp)}_3]^{2+}$ complex exhibits very high DNA binding affinity.²⁵ On the other hand Lincoln and his co-workers revealed that methyl substituents on the distant benzene ring of dppz ligand in $[\text{Ru(phen)}_2\text{11,12-dmdppz}]^{2+}$ complex substantially increases the luminescence lifetimes and quantum yields when binds to DNA.²⁶ V. Rajendiran *et. al.* studied the DNA binding mode of a series of ruthenium complexes of type $[\text{Ru(tmp)}_2/(5,6\text{-dmp})_2 \text{ (diimine)}]^{2+}$ with different diimine ligands and demonstrated that with methyl substituted diimine ligand binds to DNA more strongly than the other complexes.²⁷ R. Vilar *et.al.* have investigated that ligands containing substituents such as aromatic rings and cyclic amine, play an important role in the exhibition of the DNA binding affinity.²⁸ The interaction between ruthenium polypyridyl complexes and DNA has been studied for the last thirty years²⁹⁻³¹ because of their light switching properties and photosensitizing reactions³²⁻³³ but its detailed mode of action at the molecular level is still lacking.³⁴ Present study focuses on interaction of Ru (II) polypyridyl complexes of the type $[\text{Ru(tmp)}_2(\text{diimine})]^{2+}$ with DNA molecule in order to evaluate the information regarding the intercalative binding mode of the complexes with DNA receptors.

In principle, various techniques are available to understand the in-vitro reversible binding of metal complexes to the double-helical DNA such as spectroscopy, voltammetry and quantum chemical calculation. Indeed, molecular mechanics with improved force fields³⁵⁻³⁶ have been extensively used to analyze the structural, mechanistic and energetic properties of biomolecules. However, the molecular mechanics is not able to calculate the breaking or formation of chemical bonds. Therefore, quantum mechanical simulation has been considered for studying the interaction of biomolecules with small drug molecules. Quantum mechanical simulations can perfectly describe the hydrogen, ionic and covalent binding interactions. Unfortunately, quantum mechanical methods of high-quality are computationally very expensive and cannot be used directly for studying DNA. Hence, Morokuma and co-workers have developed a hybrid method (ONIOM) based on combination of several theoretical approaches for large biomolecular systems.³⁷⁻³⁸ ONIOM (our Own N-layer Integrated molecular Orbital molecular Mechanics) is a powerful and systematic method which divides the system into several layers. In past few years,

many researchers have utilized this powerful computational method in order to find out the stability and binding affinity of anticancer drug molecules with DNA and protein receptor.³⁹⁻⁴⁴ Recently we have used this method to explore the interaction of drug molecules with protein receptor.⁴⁵ In this study, molecular docking and ONIOM (QM/MM) method have been used to investigate the structural and energetic details of DNA duplex with $[\text{Ru}(\text{tmp})_2(\text{dpq})]^{2+}$ (**I**), $[\text{Ru}(\text{tmp})_2(\text{dppz})]^{2+}$ (**II**) and $[\text{Ru}(\text{tmp})_2(11,12\text{-dmdppz})]^{2+}$ (**III**) complexes. The mode of coordination of the ligands to Ru^{2+} is depicted in Scheme 1. In order to recognize the appropriate orientation of the metal complex into the binding site of DNA, in terms of energy, molecular docking simulations are taken up in an initial step and then quantum chemical calculations are performed using two layer ONIOM method.



Scheme1: Structure of ruthenium (II) complexes

2. Computational Details

2.1 Structure

GAUSSIAN 09 program package⁴⁶ is employed to carry out density functional theory (DFT) calculation on all the ruthenium (II) complexes using the Becke's⁴⁷ three parameter hybrid exchange functional (B3) and the Lee-Yang-Parr correlation functional (LYP) (B3LYP).⁴⁸ B3LYP functional has been used because of providing good description of reaction profiles for transition metal complexes.⁴⁹ The LANL2DZ basis set⁵⁰ which describe effective core potential of Wadt and Hay (Los Alamos ECP) on ruthenium atom and 6-311+G (d,p) basis set⁵¹ for all the non metal atoms have been used for ground state geometry optimization. The reason for using LANL2DZ basis set is that it reduces the calculation time containing larger

nuclei. The gas phase geometries of the ruthenium (II) complexes have been fully optimized using restricted B3LYP method without imposing any symmetry constraints with tight convergence criteria. Vibrational analysis has been performed at the same level of theory for achieving energy minimum.

2.2 Automated DNA— ruthenium complex docking

Molecular docking is an attractive scaffold in order to understand the Drug–DNA interactions for the rational drug design and discovery. This method is extensively used for predicting ligand conformation and its orientation in the active site of receptor. In our experiment, molecular docking studies of ruthenium(II) complexes (**I**, **II** and **III**) with DNA duplex of sequence d(ATATAT)₂ and d(GCGCGC)₂ are performed in order to find out the binding affinity and appropriate orientation of the complexes inside the DNA groove by using Auto Dock 4.2 program.⁵² Autodock 4.2 is an interactive molecular graphics program utilized to study the drug - DNA interaction.⁵³ First step of this study is to validate the docking method. The starting point is the 3D structure of a DNA duplex, d(ATGCAT)₂ which is co-crystallized with the native ligands Λ - and Δ -enantiomer of [Ru(phen)₂dppz]²⁺ (PDB code: 4e87). The crystal structure of DNA duplex d(ATGCAT)₂ is obtained from the research collaboratory for structural bioinformatics (RCSB) protein data bank whose conformation is generally B-type DNA with a low overall twist. For docking, the DNA structure in pdb format is prepared using structure preparation tool available in Auto Dock Tools package version 1.5.4. All the water molecules and the native ligand have been removed from the crystal structure of DNA and then polar hydrogen atoms have been added for saturation, Gasteiger charges are computed and non-polar hydrogen atoms are merged. Then a grid box through a grid spacing of 0.375 Å and dimension of 60×60×60 points along x, y and z axes are built around the active site of DNA. This grid box carries the complete binding site of the DNA and provides enough space for the translational and rotational movement of ligand. After that to test the validity of the docking procedure, a blind docking experiment is run on [Ru(phen)₂dppz]²⁺ (Δ -enantiomer) by selecting step sizes of 2 Å for translation and 50° for rotation. A maximum number of energy evaluations are set to 25000 and a maximum number of 27000 GA operations are generated with an initial population of 150 individuals. The rate of gene mutation and crossover are set to 0.02 and 0.80, respectively. All other parameters are kept by default. The docking experiment described above are said to be valid because we obtained the similar orientation and position of the native ligand

inside DNA receptor as reported in original X-ray crystal structure, available in the protein data bank (4e87) with an RMSD value 0.03 Å. The result of validity experiment is shown in Fig. 1. All the studied ruthenium (II) complexes are docked with the same method described above.

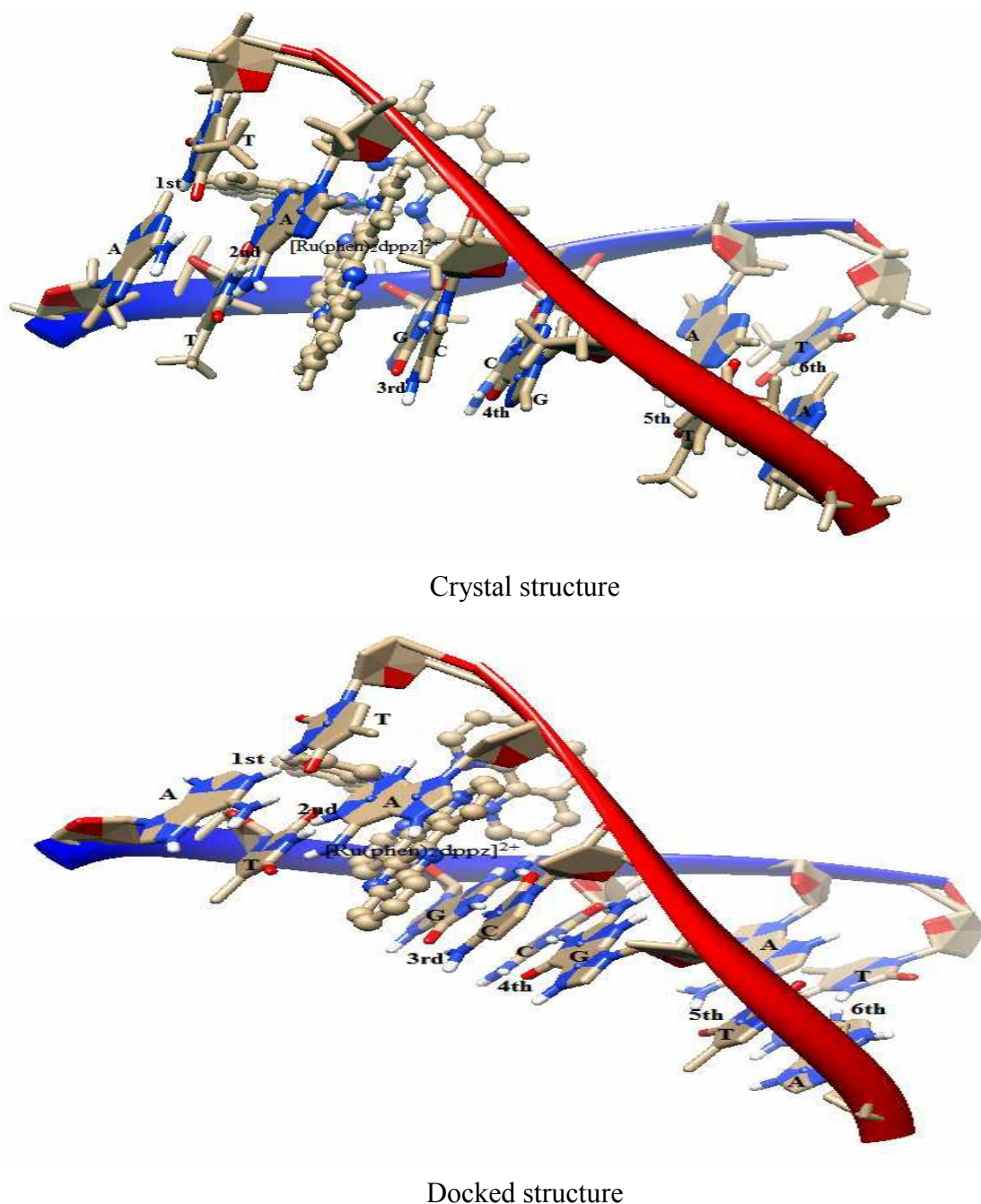


Fig.1 Docked conformation of native ligand $[\text{Ru}(\text{phen})_2\text{dppz}]^{2+}$ as compared to the conformation of ligand in the original crystal structure

2.3 Ruthenium complex-DNA interaction by QM/MM method

For performing ONIOM calculation we have considered the adduct formed between native ligand and DNA duplex d(ATGCAT)₂, as the reference point. Docking simulation shows that the native ligand intercalates into the 2nd and 3rd base pairs of DNA. Then, AT base pairs are replaced with GC base pairs from d(ATGCAT)₂ sequence to obtain d(GCGCGC)₂ and GC base pair with AT base pair to obtain d(ATATAT)₂ duplex. The DNA sequences generated are subjected to optimization by treating AT-AT and GC-GC (2nd and 3rd) base pairs (high level) with QM and remaining DNA bases and sugar-phosphate backbone (low layer) with MM in order to get a minimized energy structure. The charges of both the layer are set to be 0. RB3LYP functional with 6-311+G (d,p) basis set is used for QM layer while, UFF force field is used for the MM layer of the system.

Again docking simulation have been carried out on the ruthenium(II) complexes with energy minimized DNA structures namely d(GCGCGC)₂ and d(ATATAT)₂ and best docked structures of the complexes are selected for ONIOM calculation. The high level part (QM) includes the 2nd and 3rd base pairs of DNA along with the intercalated ruthenium complex. The charge of this layer is set to be +2. On the other hand, remaining part of DNA i.e. DNA bases, sugar-phosphate backbone are treated with MM and charge of this is set to be 0. Finally, the whole structure is optimized using two layer ONIOM method at B3LYP/ 6-311+G (d,p): UFF (QM:MM) level. All the atoms in the MM layer are kept fixed at their crystallographic location during geometry optimization. In the two layers ONIOM method, the total energy (E_{ONIOM}) of the entire system is obtained from three independent energy calculations:

$$E^{\text{ONIOM2}} = E_{\text{model system}}^{\text{high}} + E_{\text{real system}}^{\text{low}} - E_{\text{model system}}^{\text{low}}$$

Real system contains full geometry of the system and is considered as MM layer while the model system contains the chemically most important (core) part of the system that is considered as QM layer. This QM/MM computation provides a close approximation of the energy value with whole system calculated at the high-level of theory.⁵⁴⁻⁵⁵

3. Results and Discussion

3.1 Structural analysis of metal complexes

Significant optimized geometrical parameters and geometries of the ruthenium complexes **I**, **II** and **III** evaluated in gas phase at B3LYP level are presented in Table1 and Fig.2, respectively. In both the complexes, Ru²⁺ ion is octahedrally coordinated involving four

nitrogen atoms of ancillary ligands (tmp) and two nitrogen atoms of intercalating ligand (diimine). In complex **I**, the Ru—N1, Ru—N2, Ru—N3, Ru—N4, Ru—N5 and Ru—N6 bond length are calculated to be 2.113 Å, 2.116 Å, 2.116 Å, 2.115 Å, 2.106 Å and 2.096 Å, respectively, while, Ru—N5 and Ru—N6 bond lengths are found to be shorter than that of the Ru—N1, Ru—N2, Ru—N3 and Ru—N4 bond lengths, indicating the stronger coordination ability of diimine ligand (intercalating) than the tmp ligands (ancillary ligand). The bond angles N1—Ru—N2, N3—Ru—N4 and N5—Ru—N6 of the complex **I** are found to be as: 78.53°, 78.29° and 79.14°, respectively. As a consequence of this deviation of bond angles from 90°, the geometry about the ruthenium atom is distorted from regular octahedral structure. Electronic structures of all the three ruthenium complexes are found to be similar. The dihedral angle, N2—N6—N5—N3 (or N3—N5—N6—N2) as obtained from DFT is in the range of 9.36°—9.48° forming a twisted conformation of diimine with respect to the tmp moieties. Theoretical calculation shows that the diimine ligand of complexes **I**, **II** and **III** are essentially

Table1 Bond distances (Å), bond angles (⁰) and dihedral angles (⁰) of the ruthenium (II) complexes and X-ray data for [Ru(dmp)₂(dppz)]²⁺

Geometrical Parameters	Complex I	Complex II	Complex III	[Ru(dmp) ₂ (dppz)] ²⁺ (X-ray)
Ru—N1	2.113	2.114	2.113	2.110
Ru—N2	2.116	2.115	2.116	2.092
Ru—N3	2.116	2.116	2.116	2.096
Ru—N4	2.115	2.115	2.114	2.096
Ru—N5	2.106	2.106	2.106	2.073
Ru—N6	2.096	2.095	2.109	2.079
N1—Ru—N2	78.53	78.54	78.53	79.54
N3—Ru—N4	78.29	78.30	78.29	79.63
N5—Ru—N6	79.14	79.21	79.21	78.88
N2—N6—N5—N3	9.38	9.36	9.48	48.60
N3—N5—N6—N2	9.38	9.36	9.48	
N6—C6—C5—N5	-0.88	-0.64	-0.86	

planar, having dihedral angle (N6—C6—C5—N5) of -0.88° , -0.64° and -0.86° . The calculated geometrical parameters are in agreement with the similar complex $[\text{Ru}(\text{dmp})_2(\text{dppz})]^{2+}$ investigated using X-ray diffraction by Lie *et. al.*⁵⁶

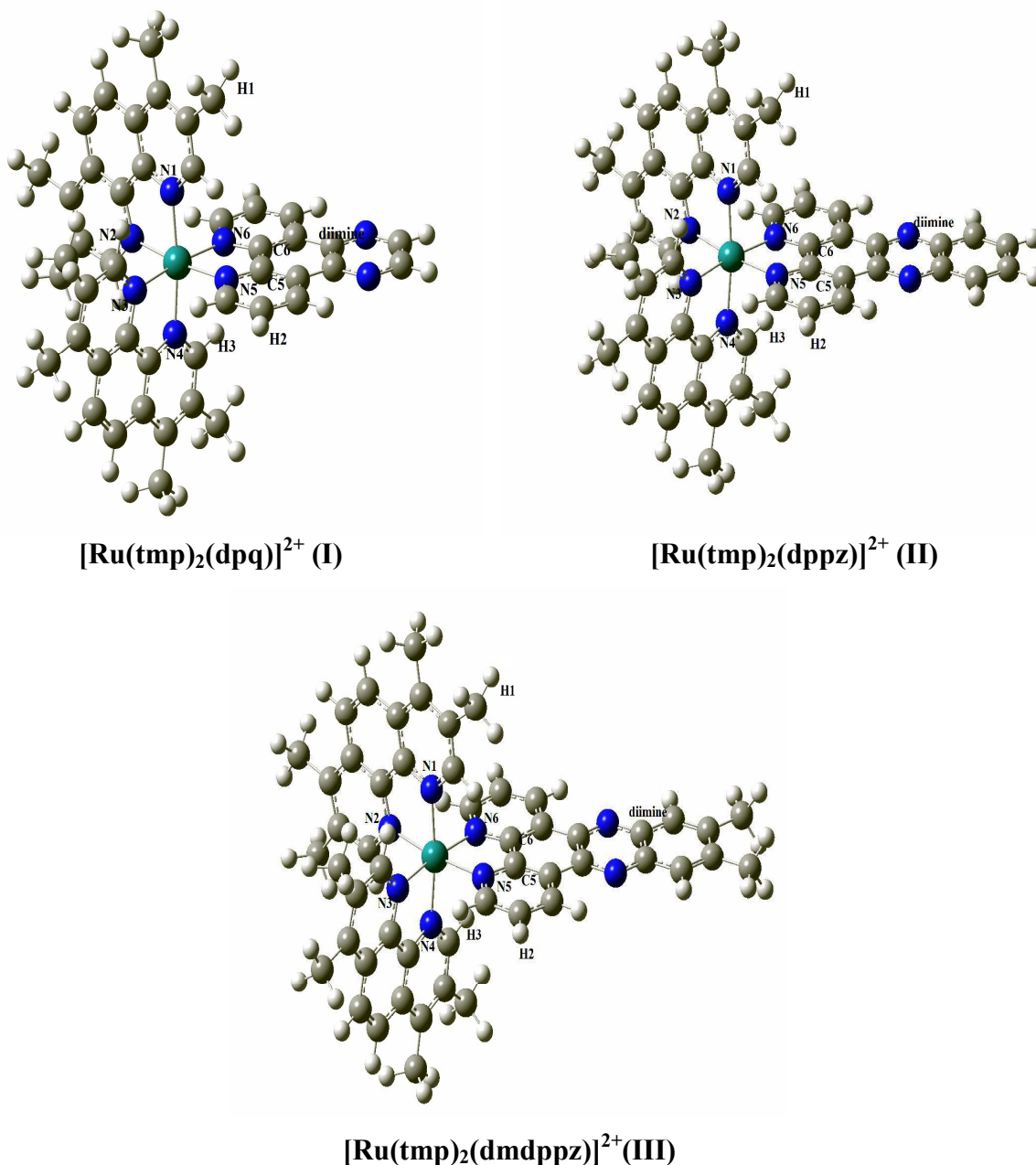


Fig.2 Optimized geometries of ruthenium (II) complexes with appropriate numbering obtained from B3LYP/ (LanL2DZ+6-311+G(d,p)) calculation.

3.2 Stability of the ruthenium complexes

Electronic properties of molecules can be determined from frontier molecular orbital⁵⁷ highest occupied molecular orbital (HOMO) and the lowest unoccupied molecular orbital (LUMO). DFT calculated LUMO and HOMO energies of the ruthenium complexes are listed in Table 2. A LUMO—HOMO energy separation of a chemical system is used to predict the kinetic stability and relative reactivity pattern. The lower value of energy separation indicates higher reactivity and lower kinetic stability of the molecules.⁵⁸ According to Pearson, LUMO—HOMO energy separation represents the chemical hardness which is a reliable reactivity parameter to predict the stability of a molecule.⁵⁹ Maximum hardness principle states that the most stable molecule has the maximum hardness value.⁶⁰ It is observed from computational investigation that complex **III** has the higher value of LUMO—HOMO energy gap, hence higher chemical hardness value. Therefore, complex **III** is found to be more stable than the other two complexes.

Table2 Energies of HOMO (E_H in eV) and LUMO (E_L in eV) and chemical hardness (η in eV) of three ruthenium (II) complexes

Complex	E_H	E_L	ΔE	η
I	-10.134	-6.818	3.316	1.658
II	-10.258	-6.896	3.362	1.681
III	-10.049	-6.653	3.396	1.698

3.3 Molecular docking study

Analysis of the molecular docking simulation shows that all the ruthenium complexes approach toward the gap between DNA minor groove mainly through diimine ligand. The relative binding energy, RMSD value and experimental binding constant (K_b in M^{-1}) values²⁷ of the studied complexes with DNA sequences (d(ATATAT)₂ and d(GCGCGC)₂) are reported in Table 3. Table 3 shows that all the complexes have exhibited RMSD value within a range 0.02-0.24 Å. The relative binding energies of the docked ruthenium complexes **I**, **II** and **III** with d(ATATAT)₂ sequence are found to be -10.88, -11.86 and -11.99 kcal mol⁻¹, whereas with d(GCGCGC)₂ sequence are found to be -8.82, -10.64 and -10.78 kcal mol⁻¹, respectively. Higher negative values of binding energy reveal stronger interaction of drug molecules with DNA. Thus

complex **III** is found to be more efficient towards DNA target as compared to the other two complexes. This finding correlates well with the experimental DNA binding data reported in the literature.²⁷ Furthermore, it has been observed that most of the minor groove binding drug molecules prefer AT rich DNA sequences rather than GC and this preferential binding leads to the better van der Waals' interaction between the drug molecules and DNA functional groups.⁶¹ Our docking result shows that interaction energy of ruthenium complexes with AT sequences are found to be higher indicating the preferential binding of these complexes with d(ATATAT)₂ sequence than that of d(GCGCGC)₂. The energetically most favorable docked conformation of complex **I** is shown in Fig. 3 and possible binding interaction of ruthenium complexes with the receptor in terms of hydrogen bonding are presented in Table 4. In the minor groove of d(ATATAT)₂ sequence, the complex **I** binds to an O atom of sugar fragment through H2 atom of diimine ligand at a distance of 2.18 Å. Another hydrogen bonding between H1 atom of ruthenium complex and O2 atom of thymine is observed at a distance of 2.28 Å. In d(GCGCGC)₂-**I**, one hydrogen bond between H2 atom of diimine ligand and oxygen atom of sugar fragment at a distance of 2.09 Å is noticed. On the other hand tmp ligand of complex **I** form hydrogen bonding with N2 atom of guanine (2.50Å) and O2 atom of cytosine (2.62Å). Similar type of bonding interactions have been observed for docking structure of complex **II** and complex **III** with respective DNA sequence which are summarized in Table 4.

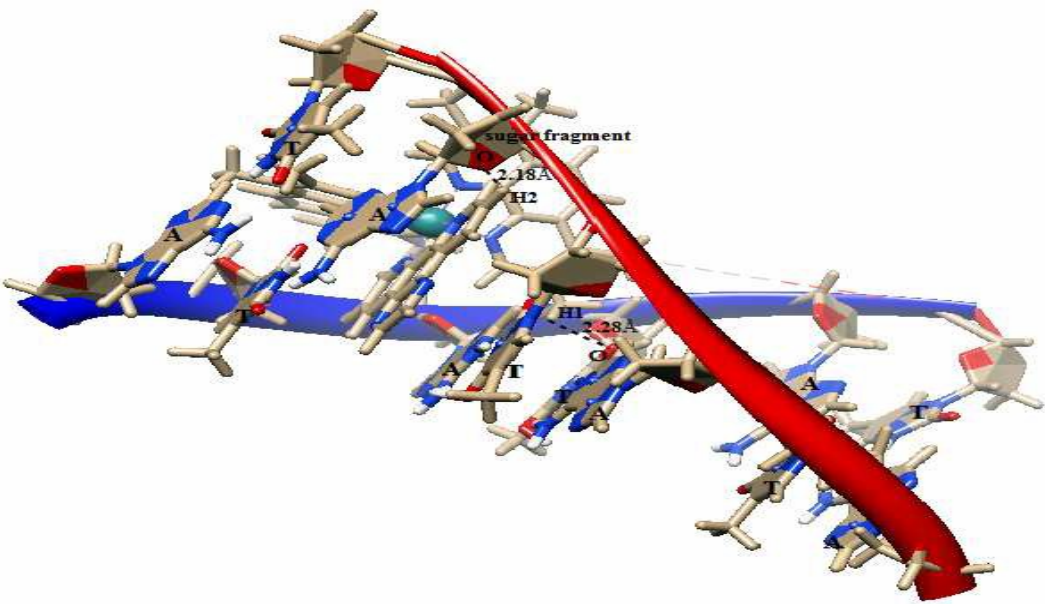
Table 3 Free energy of binding (ΔG in kcalmol⁻¹), RMSD values and intrinsic binding constant (K_b in M⁻¹) of docked structures

Metal complex	d(ATATAT) ₂		d(GCGCGC) ₂		K_b Experimental data
	(ΔG)	RMSD	(ΔG)	RMSD	
I	-10.88	0.02	-8.82	0.02	$3.0 \pm 0.2 \times 10^5$
II	-11.86	0.10	-10.64	0.14	$1.0 \pm 0.09 \times 10^6$
III	-11.99	0.05	-10.78	0.24	$6.0 \pm 0.3 \times 10^6$

Table 4 Hydrogen bond interaction of three ruthenium (II) complexes with d(ATATAT)₂ and d(GCGCGC)₂ sequences evaluated by docking analysis

Complex	H-bond	Bond	H-bond	Bond length
---------	--------	------	--------	-------------

	d(ATATAT) ₂	length	d(GCGCGC) ₂	
I	H2 of diimine: O of sugar fragment	2.18 Å	H2 of diimine: O of sugar fragment	2.09 Å
	H1 of tmp: O2 of Thymine	2.28 Å	H1 of tmp: O2 of Cytosine H3 of tmp: N2 of Guanine	2.62 Å 2.50 Å
II	H2 of diimine: O of sugar fragment	2.15 Å	H2 of diimine: O of sugar fragment	2.08 Å
	H1 of tmp: O2 of Thymine	2.18 Å	H1 of tmp: O2 of Cytosine H3 of tmp: N2 of Guanine	2.66 Å 2.50 Å
III	H2 of diimine: O of sugar fragment	2.15 Å	H2 of diimine: O of sugar fragment	2.05 Å
	H1 of tmp: O2 of Thymine	2.27 Å	H1 of tmp: O2 of Cytosine H3 of tmp: N2 of Guanine	2.65 Å 2.43 Å



d(ATATAT)₂—I

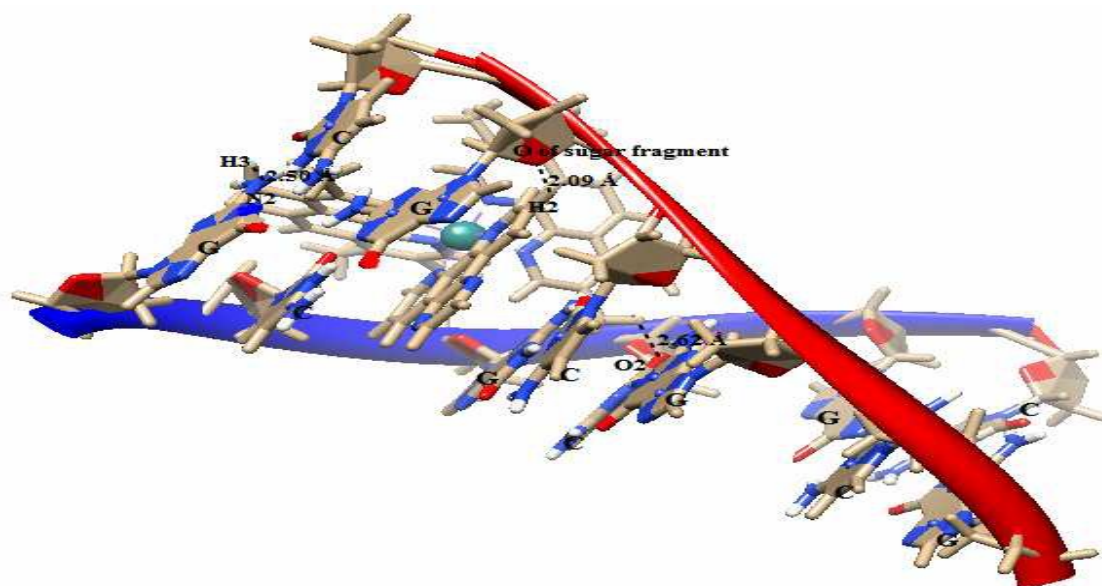


Fig.3 Docked conformation of complex **I** with d(ATATAT)₂ and d(GCGCGC)₂ sequence

3.4 QM/MM study

In this section binding energies of ruthenium complexes with DNA evaluated by QM/MM method are presented. For this purpose, best docked structure of each ruthenium complex with DNA duplex d(ATATAT)₂ and d(GCGCGC)₂ have been taken for two layer ONIOM (DFT/ RB3LYP:UFF) study. Investigation of the whole DNA with the ligand by quantum mechanics (QM) is very computationally demanding. Hence, we have applied QM on the two base pairs along with the ruthenium complex and molecular mechanics (MM) for the remaining part of the system. Fig.4 represents the optimized structures of two isolated hexanucleotide structures obtained by the two layer RB3LYP/UFF hybrid method. Results reveal that QM/MM method can properly describe the AT and GC hydrogen bonding and π — π stacking interaction of base pairs. This result is attributable for the use of the universal force field in the MM low level layer that describes the entire DNA structure. In other terms, the universal force field prevents the unphysical occurrence of axial elongation of the stacked base pairs of the intercalation site at the time of energy minimization.

The optimized structures of d(ATATAT)₂—**I** and d(GCGCGC)₂—**I** adducts are shown in Fig. 5. From Fig. 4 and Fig. 5, it is seen that the intercalation of complex **I** induces a significant distortion in DNA duplexes, compared to the conformation of isolated hexanucleotides. For monitoring the deformation of DNA duplexes at the intercalation site, the relevant structural

parameters are presented in Table 5. It is observed from Table 5 that on interaction of complex **I**, the average distance between two base pairs increases from 3.35 Å to 3.44 Å for d(ATATAT)₂ and to 3.48 Å for d(GCGCGC)₂, causing a larger axial elongation of GC—GC base pair than AT—AT base pair. Similar elongation of base pairs of DNA duplex has also been observed for complex **II** and complex **III**. Our calculation suggests that diimine ligand of ruthenium complexes are situated within the narrower AT—AT region, indicating the preferential binding of diimine moiety to AT—AT region of DNA.

On the other hand, in order to compare the relative stability of the d(ATATAT)₂—**I**, d(ATATAT)₂—**II**, d(ATATAT)₂—**III** adducts with d(GCGCGC)₂—**I**, d(GCGCGC)₂—**II**, d(GCGCGC)₂—**III** adducts, we have evaluated the binding energy, ΔE:

$$\Delta E = E_{DNA/Ru-complex} - E_{DNA} - E_{Ru-complex}$$

$E_{DNA/Ru-complex}$ is the energy of the optimized DNA/Ru-complex, E_{DNA} is the energy of the optimized DNA duplex and the $E_{Ru-complex}$ is the energy of the optimized ruthenium complexes. The binding energy values of all the ruthenium complexes with DNA are given in Table 6. Results shown in Table 6 lead us to conclude that the binding energy of ruthenium complexes with AT sequences is higher than that with GC sequences. Hence, complexes with AT sequences are more stable than with corresponding GC sequences. Again, computed binding energies of adducts **III**—d(ATATAT)₂ and **III**—d(GCGCGC)₂ are evaluated to be 222.452 kcalmol⁻¹ and 44.802 kcalmol⁻¹, respectively. These energy values are higher than that of the other adducts formed by the complexes **I** and **II** with DNA. The higher stability of the complex **III**—d(ATATAT)₂ may then be attributed to the higher π—π stacking and hydrophobic interaction of complex **III** with-d(ATATAT)₂. Due to the presence of methyl substituent on 11th and 12th position of benzene ring, complex **III** exhibits higher interaction energy. These observations are in agreement with the experimental results reported by Rajendiran *et. al.*²⁷ and Pyle *et al.*⁶²

Table 5 The structural parameters between of two AT and/or GC base pairs of DNA in free as well in complex forms.

Base pair	Base pairs stacking distance (Å)	Base pair	Base pairs stacking distance (Å)
Free AT—AT	3.35	Free GC—GC	3.35
AT— I	3.44	GC— I	3.48

AT—II	3.43	GC—II	3.42
AT—III	3.44	GC—III	3.49

Table6 The calculated binding energy (ΔE in kcalmol⁻¹) of **I**, **II** and **III** with d(ATATAT)₂ and d(GCGCGC)₂ duplex.

Complex	ΔE	
	d(ATATAT) ₂	d(GCGCGC) ₂
I	222.072	-57.005
II	222.076	-53.527
III	222.452	44.802

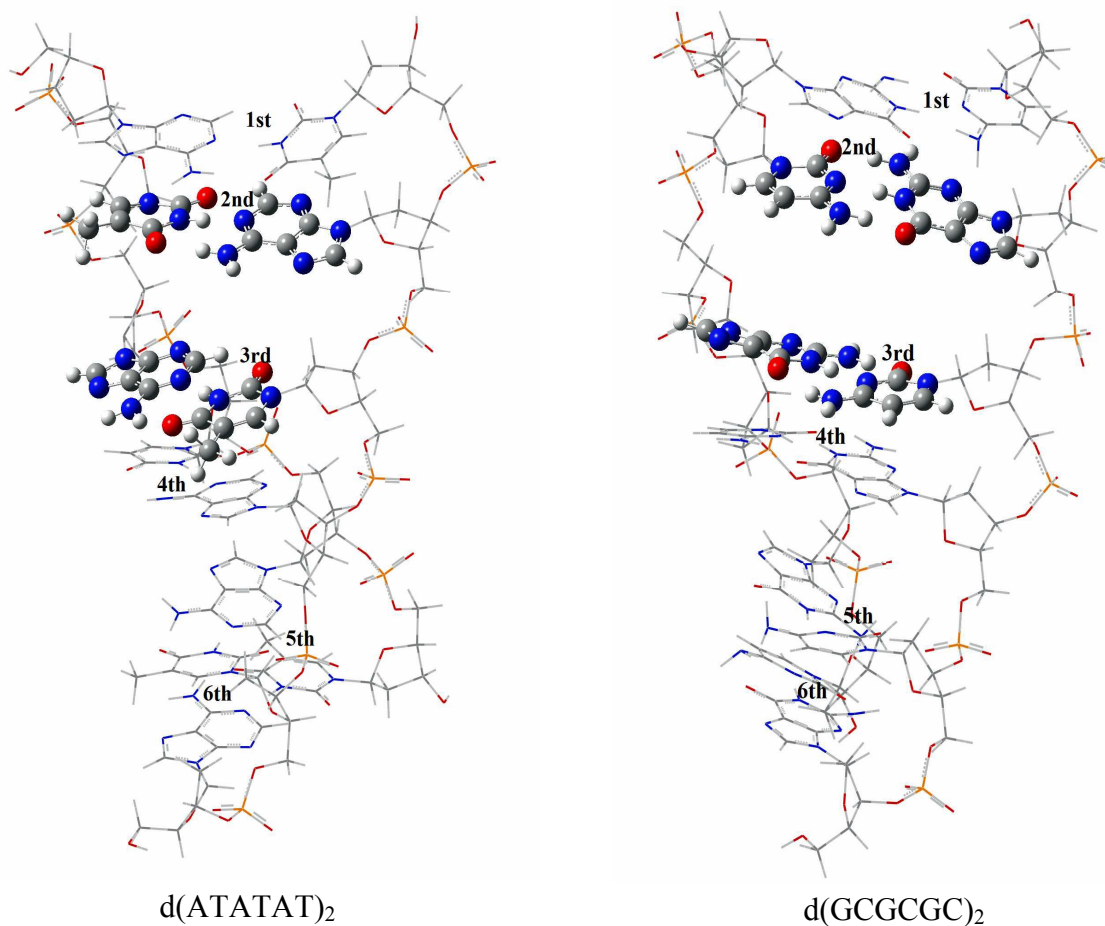


Fig.4 Optimized geometry of d(ATATAT)₂ and d(GCGCGC)₂ obtained by two layer QM/MM method

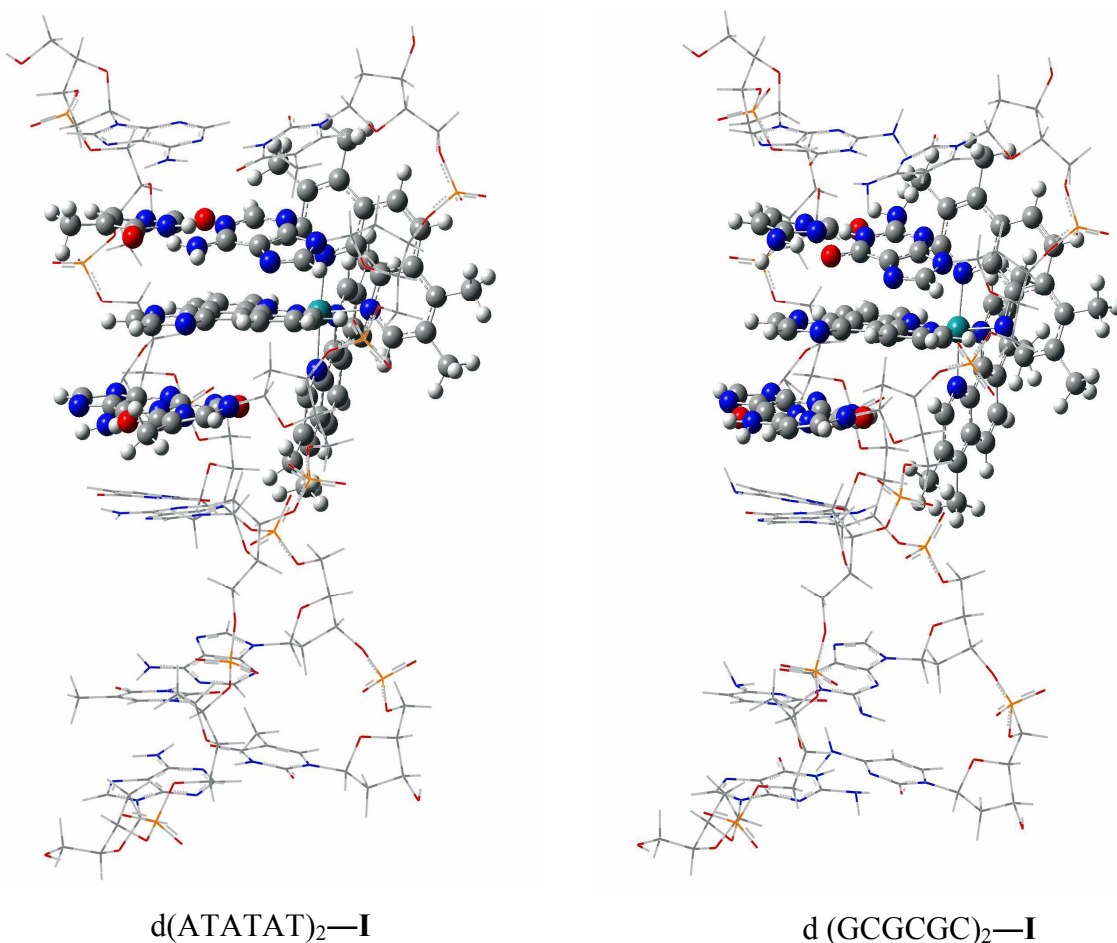


Fig.5 Optimized geometries of $d(ATATAT)_2-I$ and $d(GCGCGC)_2-I$ adducts obtained by two layer QM/MM method

4. Conclusion

Systematic molecular docking and quantum mechanics/molecular mechanics calculations have been carried out on ruthenium (II) complexes **I**, **II** and **III** in order to evaluate their binding affinity and stability towards DNA receptors. Molecular docking simulation shows that the ruthenium (II) complexes interacted in the minor groove of DNA through diimine ligand and prefer to bind to $d(ATATAT)_2$ sequence. Docking result also reveals the higher binding affinity of complex **III** towards DNA receptor in comparison to complexes **I** and **II**. Again, two layer quantum mechanics/molecular mechanics calculation on $d(ATATAT)_2$ /ruthenium(II) and $d(GCGCGC)_2$ /ruthenium(II) adducts provide atomic level structural and energetic details on the intercalated ruthenium complexes. The interaction energy evaluated by quantum mechanics/molecular mechanics calculation suggests the highest stability of complex **III** with $d(ATATAT)_2$ sequence. The higher interaction energies of ruthenium (II) complexes with AT

sequences as compared to GC sequences are well agreement with the experimental results. Interaction energy values suggest that presence of substituted aromatic ring in the intercalating ligand as well as high surface area of intercalating and ancillary ligands increases the binding affinity of the metal complex towards DNA receptor. Hence, our computed results obtained from molecular docking and quantum mechanics/molecular mechanics calculations are very encouraging in the field of drug—DNA interaction.

Acknowledgement

Author Paritosh Mondal thanks Department of Science and Technology (DST New Delhi, India) for financial support (SERB/F/1672/2013-14). Dharitri Das is thankful to the University Grants Commission (UGC), New Delhi for providing research fellowship.

References

1. A. Krishna, B. Kumar, B.M. Khan, S.K. Rawal, N. Krishna, *Biochim. Biophys. Act.*, 1998, **1381**, 104–112.
2. L. Nan, M. Ying, Y. Cheng, G. Liping, Y. Xiurong, *Biophys. Chem.*, 2005, **116**, 199–205.
3. A.M. Pizarro, P.J. Sadler, *Biochimie*, 2009, **91**, 1198–1211.
4. X.W. Liu, J. Li, H. Li, *J. Inorg. Biochem.*, 2005, **99**, 2372–2380.
5. E. Corral, C.G.A. Hotze, H. Den Dulk, *J. Biol. Inorg. Chem.*, 2009, **14**, 439–448.
6. C. Metcalfe, J.A. Thomas, *Chem. Soc. Rev.*, 2003, **32**, 215–224.
7. P.U. Maheswari, M. Palaniandavar, *J. Inorg. Biochem.*, 2004, **98**, 219–223.
8. M.S. Deshpande, A.A. Kumbhar, A.S. Kumbhar, *Inorg. Chem.*, 2007, **46**, 5450–5452.
9. K.K. Ashwini, K.L. Reddy, S. Sirasani, *Supramol Chem.*, 2010, **22**, 629–643.
10. K.L. Reddy, K.K. Ashwini, S. Sirasani, *Synth. React. Inorg. Met.- Org Nano- Met Chem.*, 2011, **41**, 182–192.
11. S. Gowda K.R., B.B. Mathew, C.N. Sudhamani, H.S.B. Naik, *Biomed. Biotech.*, 2014, **2**, 1–9.
12. D. Tilala, H. Gohel, V. Dhinoja, D. Karia, *Int. J. Chem Tech Res.*, 2013, **5**, 2329–2337.
13. J. K. Barton, K.E. Erkkila, D.T. Odom, *Chem. Rev.*, 1999, **99**, 2777–2796.
14. J. K. Barton, A. Danishefsky, J. M. Goldberg, *J. Am. Chem. Soc.*, 1984, **106**, 2172–2176.

15. M. Eriksson, M. Leijon, C. Hiort, B. Norden, B. Graeslund, *J. Am. Chem. Soc.*, 1992, **114**, 4933-4934.
16. L.S. Lerman, *J. Mol. Biol.*, 1961, **3**, 18-30.
17. A.E. Friedman, J.C. Chambron, J.P. Sauvage, N.J. Turro, J.K. Barton, *J. Am. Chem. Soc.*, 1990, **112**, 4960–4962.
18. Y. Jenkins, A.E. Friedman, N.J. Turro, J.K. Barton, *Biochemistry*, 1992, **31**, 10809–10816.
19. C.M. Dupureur, J.K. Barton, *J. Am. Chem. Soc.*, 1994, **116**, 10286-10287.
20. C.M. Dupureur, J.K. Barton, *Inorg. Chem.*, 1997, **36**, 33-34.
21. H. Song, J. T. Kaiser, J. K. Barton, *Nat. Chem.*, 2012, **4**, 615-620.
22. J. Andersson, L. H. Fornander, M. Abrahamsson, E. Tuite, P. Nordell, P. Lincoln, *Inorg. Chem.*, 2013, **52**, 1151–1159.
23. J. P. Hall, D. Cook, S. R. Morte, P. McIntyre, K. Buchner, H. Beer, D.J. Cardin, J. A. Brazier, G. Winter, J. M. Kelly, C. J. Cardin, *J. Am. Chem. Soc.*, 2013, **135**, 12652–12659.
24. K.E. Erkkila, D.T. Odom, J.K. Barton, *Chem. Rev.*, 1999, **99**, 2777–2795..
25. K. Maruyama, J. Motonaka, Y. Mishima, Y. Matsuzaki, I. Nakabayashi, Y. Nakabayashi, *Sensor Act. B*, 2001, **76**, 215–219.
26. J. Olofsson, L. M. Wilhelmsson, P. Lincoln, *J. Am. Chem. Soc.*, 2004, **126**, 15458-15465.
27. V. Rajendiran, M. Palaniandavar, V. S. Periasamy, M. A. Akbarsha, *J. Inorg. Biochem.*, 2012, **116**, 151–162
28. V. S. Stafford, K. Suntharalingam, A. Shivalingam, A. J. P. White, D. J. Mann, R. Vilar, *Dalton Trans.*, 2014, DOI: 10.1039/c4dt02910k.
29. R.M. Hartshor, J.K. Barton, *J Am. Chem. Soc.*, 1992, **114**, 5919–5925.
30. J.G. Vos, J.M. Kelly, *Dalton Trans.*, 2006, **41**, 4869–4883.
31. B. Elias, A. Kirsch-De Mesmaeker, *Coord. Chem. Rev.*, 2006, **250**, 1627–1641.
32. J.M. Kelly, A.B. Tossi, D.J. McConnell, C.A. O'hUigin, *Nucleic Acids Res.*, 1985, **13**, 6017–6034.
33. J.K. Barton, *Science*, 1986, **233**, 727–734.

34. A. Mukherjee, R. Lavery, B. Bagchi, *J. Am. Chem. Soc.*, 2008, **130**, 9747–9755.
35. F. Ahmadi, N. Jamali, R. Moradian, B. Astinchap, *DNA Cell Biol.*, 2012, **31**, 259–268.
36. F. Ahmadi, N. Jamali, S. Jahangard-Yekta, B. Jafari, S. Nouri, F. Najafi, M. Rahimi-Nasrabadi, *Spectro. Chim. Acta A*, 2011, **79**, 1004-1012.
37. K.J. Morokuma, *Bull. Korean Chem. Soc.*, 2003, **24**, 797–801.
38. S. Dapprich, I. Komáromi, K. Suzie Byun, K.J. Morokuma, M.J. Frisch, *J. Mol. Struct. Theochem.*, 1999, **461–462**, 1–21.
39. T. Yoshida, Y. Munei, S. Hitaoka, H. Chuman, *J. Chem. Inf. Model.*, 2010, **50**, 850–860.
40. J. H. Alzate-Morales, J. Caballero, F. D. Gonzalez-Nilo, R. Contreras, *Chem. Phys. Lett.*, 2009, **479**, 149-155.
41. J. H. Alzate -Morales , J. Caballero, A. V. Jague, F. D. Gonzalez -Nilo, *J. Chem. Inf. Model.*, 2009, **49**, 886–899.
42. K. Gkionis, S. T. Mutter , J. A. Platts, *RSC Adv.*, 2013, **3**, 4066-4073.
43. Z. Futera, J. V. Burda, *J. Comput. Chem.*, 2014, **35**, 1446–1456.
44. Z. Futera, J.A. Platts, J.V. Burda, *J. Comput. Chem.*, 2012, **33**, 2092-20101.
45. D. Das, A. Dutta, P. Mondal, *RSC Adv.*, 2014, **4**, 60548–60556.
46. M. J. Frisch, G. W. Trucks, H. B. Schlegel, G. E. Scuseria, M. A. Robb, J. R. Cheeseman, G. Scalmani, V. Barone, B. Mennucci, G. A. Petersson, H. Nakatsuji, M. Caricato, X. Li, H. P. Hratchian, A. F. Izmaylov, J. Bloino, G. Zheng, J. L. Sonnenberg, M. Hada, M. Ehara, K. Toyota, R. Fukuda, J. Hasegawa, M. Ishida, T. Nakajima, Y. Honda, O. Kitao, H. Nakai, T. Vreven, J. A. Montgomery, J. E. Peralta, F. Ogliaro, M. Bearpark, J. J. Heyd, E. Brothers, K. N. Kudin, V. N. Staroverov, T. Keith, R. Kobayashi, J. Normand, K. Raghavachari, A. Rendell, J. C. Burant, S. S. Iyengar, J. Tomasi, M. Cossi, N. Rega, J. M. Millam, M. Klene, J.E. Knox, J. B. Cross, V. Bakken, C. Adamo, J. Jaramillo, R. Gomperts, R. E. Stratmann, O. Yazyev, A. J. Austin, R. Cammi, C. Pomelli, J. W. Ochterski, R. L. Martin, K. Morokuma, V. G. Zakrzewski, G. A. Voth, P. Salvador, J. J. Dannenberg, S. Dapprich, A. D. Daniels, O. Farkas, J. B. Foresman, J. V. Ortiz, J. Cioslowski and D. J. Fox, Gaussian 09 (Revision B.01), Gaussian Inc., Wallingford, CT, 2010.
47. A. D. Becke, *Phys. Rev. A*, 1988, **38**, 3098-3100.
48. C. Lee, W. Yang, R. G. Parr, *Phys. Rev.*, 1988, **37**, 785-789.

49. R.J. Nielsen, J.M. Keith, B.M. Stoltz, W.A. Goddard, *J. Am. Chem. Soc.*, 2004 **126**, 7967-7974.
50. P. J. Hay, W. R. Wadt, *J. Chem. Phys.*, 1985, **82**, 270-284.
51. P. C. Hariharan, J. A. Pople, *Chem. Phys. Lett.*, 1972, **16**, 217-219.
52. G. M. Morris, R. Huey, W. Lindstrom, M. F. Sanner, R. K. Below, D. S. Goodsell, A. Olson J, *J. Comput. Chem.*, 2009, **30**, 2785-2791.
53. A. Robertazzi, A. Vittario Vargiu, A. Magistrato, P. Ruggerone, P. Carloni, P. D. Hoog, J. Reedijk, *J. Phys. Chem. B*, 2009, **113**, 10881-10890.
54. M. Svensson, S. Humbell, R.D.J. Froese, T. Matsubara, S. Sieber, K. Morokuma, *J. Phys. Chem.*, 1996, **100**, 19357.
55. T. Vresen, K. Morokuma, *J. Comput. Chem.*, 2001, **21**, 1419.
56. J.G. Liu, Q.L. Zhang, X.F. Shi, L.N. Ji, *Inorg. Chem.*, 2001, **40**, 5045-5050.
57. I. Fleming, *Frontier orbitals and organic chemical reactions*, London, Wiley, 1976.
58. J.I. Aihara, *J. Phys. Chem. A*, 1999, **103**, 7487-7495.
59. R. G. Pearson, *Hard and soft acids and bases*, Dowden, Hutchinson, Ross, Stroudsburg, PA, 1973.
60. R.G. Pearson, *J. Chem. Educ.*, 1987, **64**, 561-567.
61. R. Filosa, A. Peduto, S. Di Micco, P. de Caprariis, M. Festa, A. Petrella, G. Capranico, G. Bifulco, *Bioorg. Med. Chem.*, 2009, **17**, 13-24.
62. A.M. Pyle, J.K. Barton, *Prog. Inorg. Chem.*, 1990, **38**, 413-475.